

# APPENDIX B

## B.1 Analysis of Possible Blood Cell Collision Models for Dense Suspensions

### B.1.1 Introduction

As discussed in the literature review, the motion of individual particles in blood flow is directly influenced by hydrodynamic interactions with other cells. In suspensions of rigid spheres, experiments have determined that shear-induced particle self-diffusion in a region of constant concentration scales linearly with shear rate and the square of particle radius (Eckstein et al., 1974; Leighton and Acrivos, 1987). For rigid spheres, Leighton and Acrivos (1987) suggested that in the presence of a concentration gradient there is a nonrandom particle drift (persistent motion) across streamlines, which is proportional to particle concentration, viscosity, shear rate, and their respective gradients. It is this non-random drift, or source term, that is responsible for non-uniform particle concentration profiles under fully developed conditions. The effect of this nonrandom drift is reportedly much larger than shear-induced particle dispersion only (Leighton and Acrivos, 1987).

In blood flow, hydrodynamic interactions are dominated by red blood cells, which account for 99% of the particle phase by volume. The effect of various shear conditions on the local concentration of red blood cells is of interest. In a dilute suspension, flexible red blood cells migrate down a shear gradient at a rate much greater than would be observed for rigid spheres (i.e., Segre-Silberberg effect as summarized by Brenner (1966)) undergoing Saffman lift (Goldsmith and Turitto, 1986). However, in a dense suspension the inward migration is severely impeded by particle-particle interactions. Furthermore, as discussed in the literature review, red blood cell motion and interaction is significantly influenced by the magnitude of the shear applied. For example, at low shear rates, a red blood cell tumbles like a solid; at intermediate shear rates, it exhibits drop-like deformation; and at high shear stresses, the membrane circulates about the particle center, i.e., tank treading motion

(Goldsmith and Turitto, 1986). Experimental observations of red blood cell concentration profiles developing in tube flow reveal that red blood cells lift off the wall essentially upon entry in the tube. Thereafter, a slow development of the red cell concentration profile continues over many tube diameters (Carr, 1989). Apparently, an accurate solution to the problem of red blood cell motion in a concentrated suspension must address events on a small time scale (to account for rapid off-wall motion) and be applicable at very large times (as is required for the simulation of fully developed concentration profiles).

Two approaches have previously been applied to determine the influence of red blood cell interaction on blood particle motion. To address small time scale issues, the near instantaneous lateral motion of platelets and white blood cells have been measured for various hematocrits at shear rates less than  $20 \text{ s}^{-1}$ . However, because the underlying mechanism for lateral blood particle motion (i.e. red blood cell interaction) does not behave linearly with shear, it is unlikely that a dispersion coefficient,  $D_p$ , will linearly scale with shear beyond  $\dot{\gamma} = 20 \text{ s}^{-1}$ . Comparatively, the development of concentration profiles requires a much larger time scale, e.g., the results of Eckstein and Belgacem (1991) indicate that platelet concentration is still changing significantly 10,000 diameters downstream in a narrow tube. The second approach to determine the influence of red blood cells on critical particle motion is referred to as the drift flux model. As discussed in the literature review, the drift flux approach of Eckstein and Belgacem (1991) is severely limited to the exact system for which it was derived. An extension of this model provided by Buchanan and Kleinstreuer (1998) has similar limitations. A more general model applicable to a wide range of time scales was derived by Phillips et al. (1992) to simulate the lateral motion of rigid spheres.

### B.1.2 Attempted Models

Due to a lack of experimental evidence regarding monocyte and platelet dispersion and drift at physically relevant shear rates, considerable effort was made to deduce a collision model from available data in the literature. The general premise of the model was that platelet and monocyte dispersion should be a function of both local red blood cell concentration ( $h$ ) and shear rate ( $\dot{\gamma}$ ). The volume fraction of spherical solid particles will be

denoted  $\phi$  while the volume fraction of red blood cells, i.e., the local hematocrit, will be denoted  $h$ . The first step in such a model is to estimate the local hematocrit, i.e., determine red blood cell concentration profiles on a Eulerian basis. Because closure conditions are not present for a two-fluid model of red blood cell motion, and due to the low Stokes number, it seems logical to instead use a flow mixture model supplemented with derived coefficients. Such a model is available for spherical particles (Phillips et al., 1992; Hofer and Perktold, 1997). However, due to complications introduced by the flexible nature of red blood cells, a feasible model for red blood cell concentration could not be determined. Outlined below are details of a variety of attempts to model red blood cell concentration profiles on a Eulerian basis and a brief description of why the models failed. Shear rate based models for platelet and monocyte dispersion that assume a mean red blood cell concentration are then discussed.

*Flux Terms of Leighton and Acrivos (1987)*

*Background.* Phillips et al. (1992) modified and applied concepts suggested by Leighton and Acrivos (1987) to develop a diffusion equation that describes the evolution of particle concentration profiles in shear flow. This model is applicable for rigid spherical particles of volume fraction  $0.0 < \phi < 0.68$  and large particle Peclet numbers, i.e.,

$$Pe = \frac{a^2 \dot{\gamma}}{D_s} \gg 1 \quad (\text{B.1})$$

where  $a$  is the particle radius and  $D_s$  is the thermal diffusivity. The resulting constitutive relation is second-order and nonlinear with respect to the particle volume fraction, and can be solved in conjunction with the equations of motion.

To model particle interaction, Phillips et al. (1992) derived semi-empirical expressions for lateral particle flux via the two mechanisms discussed by Leighton and Acrivos (1987a). One of these Eulerian flux terms accounts for migration of particles from a region of high particle-to-particle collision rate to a region of lower interaction. The other flux term is due to the fact that an interaction between two particles will be affected by the spatially varying viscosity (caused by the existence of gradients in the particle concentration). These flux terms are proportionalities and require correction via empirically derived

constants. Phillips et al. (1992) went on to determine these constants for rigid spheres in Couette and Poiseuille flows.

*Extension.* Appropriate coefficients for a fully developed profile of red blood cell concentration could not be determined for the flux terms. This is due to the fact that a single viscosity relation

$$\eta = \eta(\phi) \tag{B.2}$$

exists for hard spheres but not for flexible red blood cells. In the hard sphere model, Eq. (B.2) served to limit the maximum concentration of spheres. For red cells, we instead have

$$\eta = \eta(\dot{\gamma}) \quad \text{at } \bar{h} \tag{B.3}$$

where different relations exist for various values of  $\bar{h}$ . Applying Eq. (B.3) provided no means to limit the local value of particle concentration. Therefore, a large flux term in the near-wall region (required to capture small time scale effects) resulted in concentrations much larger than physically possible near the tube center. Attempts to derive an expression<sup>1</sup>

$$\eta = \eta(h) \quad \text{at } \dot{\gamma} \tag{B.4}$$

for red blood cells were to no avail due to the flexible nature of the cells. That is, such a relation would only be valid for a certain shear rate and would be extremely sensitive to variation in shear.

#### *Drift Flux Model of Eckstein and Belgacem (1991)*

*Background.* The drift flux model of Eckstein and Belgacem (1991) uses a source term to account for the nonrandom drift induced by particle concentration gradients over a long period of time, as discussed in the literature review. The source, or drift term is determined as a derivative of the fully developed particle concentration profile for that system, i.e., the profile to be determined. There is no theoretical basis for extending the drift term of Eckstein and Belgacem (1991) to a system other than the one for which it was derived, i.e., shear rate, platelet concentration, local hematocrits, and geometry cannot be varied.

---

<sup>1</sup> It is noted that such a relation could be directly used to find red blood cell concentration owing to the fact that we already have an accurate prediction of local viscosity.

*Extension.* If we could derive a drift term proportional to physically relevant constants, such as viscosity and shear rate, a generalized model would result. Unfortunately, no combination of  $\eta, \dot{\gamma}, \frac{d\eta}{dr}, \frac{d\dot{\gamma}}{dr}$  could be found that would result in fully developed red blood cell or platelet concentration profiles. Nonlinear regression techniques in MathCAD were implemented to search for the appropriate combination. Difficulties arose due to the fact that the shear rate is nearly linear and the viscosity varies by several orders of magnitude.

### *A Variable Hematocrit Approach Based on Experimental Evidence*

*Background.* Zydney and Colton (1988) compiled a number of dispersion coefficients for red blood cells at various mean hematocrits; all of which were measured below a shear rate of  $20 \text{ s}^{-1}$ . The resulting equation is

$$\frac{D_p}{a_p^2 \dot{\gamma}} = kh(1-h)^n \quad (\text{B.5})$$

where  $a_p$  is the particle radius and  $k$  and  $n$  are constants that are to be determined. Equation (5) is plotted in Figure B.1.

*Extension.* The idea is that Eq. (B.5) can be applied at a local level to determine the dispersion coefficient for red blood cells or for platelets. The simulation of fully developed red blood cell concentration profiles in a tube was first investigated.

The diffusion equation in cylindrical coordinates is

$$\frac{\partial h}{\partial t} = \frac{a^2}{r} \frac{\partial}{\partial r} \left\{ r D_p \frac{\partial h}{\partial r} \right\} \quad (\text{B.6})$$

Using Equation (6) with no sources (or sinks) a fully developed profile, i.e., when the concentration is no longer changing with time, is always a constant valued function. However, we want to substitute Eq. (B.5) into Eq. (B.6) to simulate the experimentally observed parabolic-like concentration profiles. This may be possible if we speculate that there exists a large range in time,  $\hat{t}$ ,

$$t_o \ll \hat{t} \ll t_\infty \quad (\text{B.7})$$

for which the profile is effectively constant.

Substituting Eq. (B.5) into Eq. (B.6) results in

$$\frac{\partial h}{\partial t} = \frac{a^2}{r} \frac{\partial}{\partial r} \left\{ r \dot{\gamma}(r) k h(1-h)^n \frac{\partial h}{\partial r} \right\} \quad (\text{B.8})$$

which has a variable coefficient and is highly nonlinear. The idea is that particles will diffuse almost linearly with shear rate and with  $h$  until around  $h \cong 0.5$ , cf. Fig. B.1, at which point diffusion becomes limited by local concentration.

The solution of Eq. (B.8) is complicated due to the nonlinear nature of the diffusion term. Furthermore, Eq. (B.8) is in non-conservative form owing to the  $1/r$  term outside the derivative terms. Due to the non-conservative nature, a finite difference technique will most likely introduce erroneous sources or sinks. Therefore, a finite volume technique is a better approach.

Using CFX 4.4 to solve Eq. (B.8) revealed that the values of  $D_p$  were insufficient to capture the rapid off wall motion reported by experimental observations at  $\dot{\gamma}_w = 240 \text{ s}^{-1}$ . This was determined beforehand from an order of magnitude analysis that indicates typical  $D_p$  values predicted by equation (B.5) are on the order of  $10^{-6} \text{ cm}^2/\text{s}$ . Assuming uniform dispersion, i.e.,

$$\Delta r^2 = 2D_p \Delta t, \quad (\text{B.9})$$

it is clear that a considerable amount of time is required for any appreciable lateral motion of red blood cells away from the wall. It seems likely that at shear rates above  $\dot{\gamma} = 20 \text{ s}^{-1}$  (i.e.,  $\dot{\gamma} = 20 \text{ s}^{-1}$  was the maximum shear rate considered in deriving Eq. (B.5))  $D_p$  scales more strongly than linearly with  $\dot{\gamma}$ , e.g.,

$$D_p \sim a^2 \dot{\gamma}^m, \quad (\text{B.10})$$

for red blood cell dispersion. However, this relationship only holds true to some maximum shear rate. In fact, Yeh and Eckstein (1994) observed red blood cell induced lateral transport was reduced somewhere beyond  $\dot{\gamma} = 560 \text{ s}^{-1}$ .

### B.1.3 Conclusions Regarding a Red Blood Cell Dispersion Model

The dispersion coefficient deduced from Eq. (B.5) with the inclusion of Eq. (B.10) may be a viable way to simulate red blood cell concentration profiles. However, considerable effort will be required just to match steady state profiles, i.e., three constants must be determined. Once these constants have been determined, there is no guarantee that the third constant ( $m$ ) will be capable of simulating the small time scale phenomena<sup>2</sup>. Instead, at this point it is more logical to refocus on the actual motion of platelets and monocytes over a small time scale assuming that the variable red blood cell concentration field can be approximated as

$$h(r) \cong \bar{h} \quad (\text{B.11})$$

For this case, diffusion coefficients have been computed by Goldsmith and Marlow (1979) for  $\dot{\gamma} < 20 \text{ s}^{-1}$ , as in Fig. B.2. A wealth of information is available for platelet diffusion in a shear field beyond  $\dot{\gamma} = 20 \text{ s}^{-1}$  and agrees with the above measurements in the low shear range as, summarized below. Unfortunately, few experiments have been conducted regarding monocyte dispersion at physically relevant shear rates and Reynolds numbers.

## B.2 Effective Dispersion Coefficients

### B.2.1 Shear Rate Models for Platelet Dispersion

As discussed in the literature review, a result of some *in vitro* platelet deposition experimental models has been an estimate of the enhanced diffusion of platelets modeled as a chemical species or solute. Grabowski et al. (1972) estimated platelet diffusivity by fitting a species transport model of platelet deposition to experimental measurements of canine platelet deposition on glass surfaces. Other investigators used the same approach with different experimental data. Turitto and Baumgartner (1975) used *in vitro* measurements of rabbit platelet deposition on rabbit sub-endothelium in an annular chamber. Enhanced diffusivity was fit to a power law

---

<sup>2</sup> The original motivation behind using Eq. (5) was that it had been derived from instantaneous red blood cell motion. Therefore, to first order, small time scale motion could be assumed to be implicit.

$$D_e = a \dot{\gamma}_w^n \quad (\text{B.12})$$

where  $\dot{\gamma}_w$  is the shear rate at the surface and  $D_e$  is the effective solute diffusion coefficient. The shear rates in these experiments ranged from 10 to 832  $\text{s}^{-1}$ . The power that best fit the experimental data was usually around 0.5 to 0.6. The main difficulty with these experiments is the interdependence between the estimated diffusivity and the effective kinetic rate of platelet deposition, which is probably also a function of shear rate (Turitto et al., 1980). That is, the estimated constants are calculated based on measured platelet deposition.

Nevertheless, results are similar for a wide array of highly reactive surfaces indicating that platelet attachment is diffusion controlled for shear rates below  $\dot{\gamma} = 800 \text{ s}^{-1}$ , as shown by Turitto et al. (1980). Both Turitto et al. (1980) and Wootton et al. (1998) implemented Eq. (B.12) in a chemical species model of platelet transport. Such models generally depend on boundary layer assumptions to determine platelet flux expressions. In regions where boundary layer theory fails, e.g., in separated flow, such models are typically not valid.

In order to apply Eq. (B.12) to the motion of individual platelets, the reported solute diffusivity,  $D_e$ , must be converted to a particle dispersion coefficient,  $D_p$ . Zydney and Colton (1988) showed that if particle rotation is assumed unimportant

$$D_e = D_s + D_p \quad (\text{B.13})$$

where  $D_s$  is the thermal diffusivity of the solute. Realizing that  $D_s$  is two orders of magnitude less than  $D_p$  even in very low shear flow (Goldsmith and Turitto, 1986) allows for the approximation

$$D_p \approx D_e \quad (\text{B.14})$$

Assuming the process to be Gaussian, the mean lateral dispersion is given by Eq. (B.9), i.e.,

$$\Delta r = \sqrt{2D_p \Delta t} \quad (\text{B.15})$$

Individual displacements can be calculated using random walk theory as with Balashazy (1993), i.e., a Monte Carlo type approach. The above approximations do not consider red blood cell concentration gradients and, therefore, do not allow for the persistent motion that results in the appropriate concentration profiles over a large time scale. Nevertheless, such approximations should be appropriate over small time scales, i.e., on the order of ten tube diameters, if we begin with the correct particle distribution profile.

While Eq. (B.12) has been widely used, Aarts et al. (1986) have more recently calculated platelet diffusivity over a wider range of shear rates and included the effect of hematocrit. Using the *in vitro* experimental arrangement of Turitto and Baumgartner (1975), Aarts et al. (1986) estimated platelet diffusion by measuring platelet deposition on sub-endothelial tissue over a shear rate range of  $200 \text{ s}^{-1}$  to  $1300 \text{ s}^{-1}$ , i.e., the region of diffusion controlled deposition. The maximum mean hematocrit studied was  $\bar{h} = 0.6$ . The resulting correlation was

$$D_e = 1.05 \times 10^{-9} \dot{\gamma}^{0.297+1.29\bar{h}-0.90\bar{h}^2} \quad (\text{B.16})$$

where  $\bar{h}$  is the mean hematocrit and  $\dot{\gamma}$  is the local shear rate. The resulting values for platelet diffusivity ranged from  $0.4$  to  $1.3 \times 10^{-7} \text{ cm}^2/\text{s}$  at  $\bar{h} = 0.4$ , as illustrated in Fig. B.3. The correlation of Aarts (1986) is far more versatile than Eq. (B.12) and will, therefore, be used to estimate platelet dispersion under the assumption of a constant mean red blood cell distribution<sup>3</sup>, i.e., Eq. (B.11). As discussed above, Eq. (B.14) can be used to estimate the particle dispersion coefficient and a random walk simulation can be used to determine individual particle trajectories.

### B.2.2 Shear Rate Model for Monocyte Dispersion

Monocytes are larger than platelets and cannot typically be modeled as a solute such that mass transport theory can be used to estimate their effective diffusivity. Instead, monocyte dispersion coefficients must be measured directly by investigating the traces of individual cells moving in a shear field. Traces of leukocyte dispersional displacements are presented in Goldsmith and Karino (1974) and resemble red blood cell motion. From these measurements, a dispersion coefficient for white blood cell transport can be estimated as

$$D_p = 1.5 \times 10^{-7} \text{ cm}^2 / \text{s} \quad (\text{B.17})$$

at an approximate shear rate of  $20 \text{ s}^{-1}$  where  $\bar{h} = 0.4$ . This dispersion coefficient concurs in magnitude with observations of Eckstein and Leggas (1999). Unfortunately, higher shear

---

<sup>3</sup> Should a model for red blood cell concentration become available, Eq. (16) can be applied using the local red blood cell concentration to estimate a more accurate description of platelet motion over time.

estimates of monocyte dispersion are not available. A conservative assumption regarding monocyte dispersion is that it is shear independent at a particular mean hematocrit. Alternatively, a variable dispersion coefficient can be estimated by considering that red blood cell interactions influence both platelet and monocyte dispersion. Due to the underlying mechanism of red blood cell interaction, it is proposed that monocytes will be dispersed in a shear dependent manner similar to platelets. Using the mean hematocrit assumption, i.e., Eq. (B.11), monocyte dispersion coefficients can be fit to a model similar to Eq. (B.12). Possible results are indicated in Fig. B.4. Experiments that track the motion of individual monocytes will be necessary to determine the coefficients for such a dispersion model (e.g., as with Goldsmith and Turitto, 1986; Eckstein and Leggas, 1999).

### B.2.3 Summary

In conclusion, the dispersion of critical blood elements will be assumed to occur at a constant mean hematocrit. Due to the excessively low Stokes number of platelets, a wealth of solute diffusion experiments can be converted to particle dispersion coefficients. In particular, a broad correlation by Aarts et al. (1986) is the most general experimental relation for the diffusion of platelets. With respect to monocytes, only low shear dispersion estimates are available. A constant estimate of white blood cell dispersion is the most justifiable assumption. A parametric sensitivity analysis can be conducted to determine the consequences of this assumption.

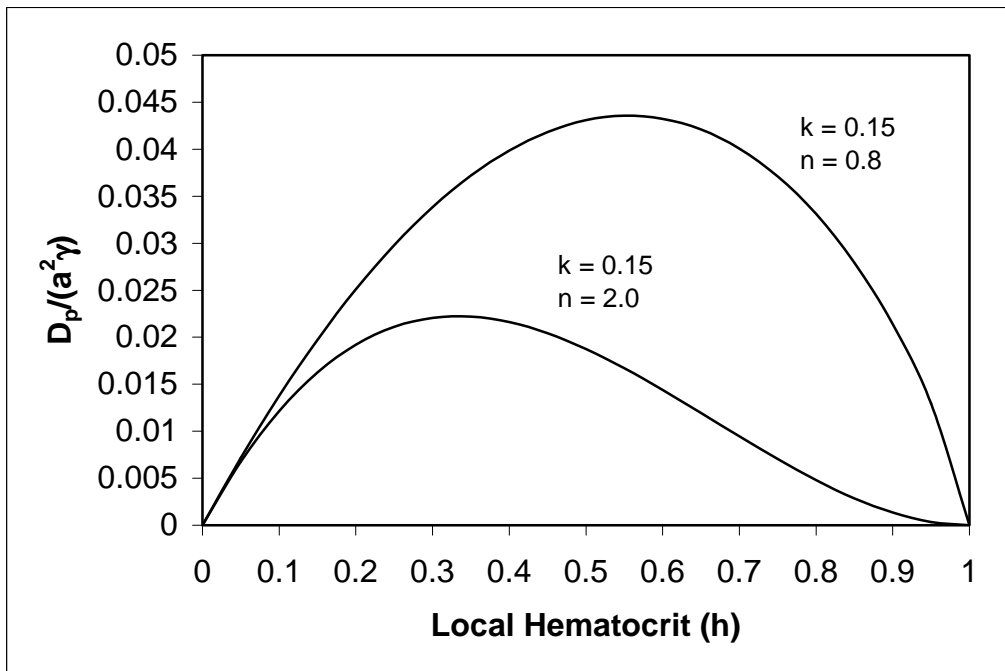


Figure B.1. Correlation of Zydney and Colton (1988) for red blood cell dispersion. Case of  $k = 0.15$  and  $n = 0.8$  results from experimental data,  $\dot{\gamma} < 20 \text{ s}^{-1}$ .

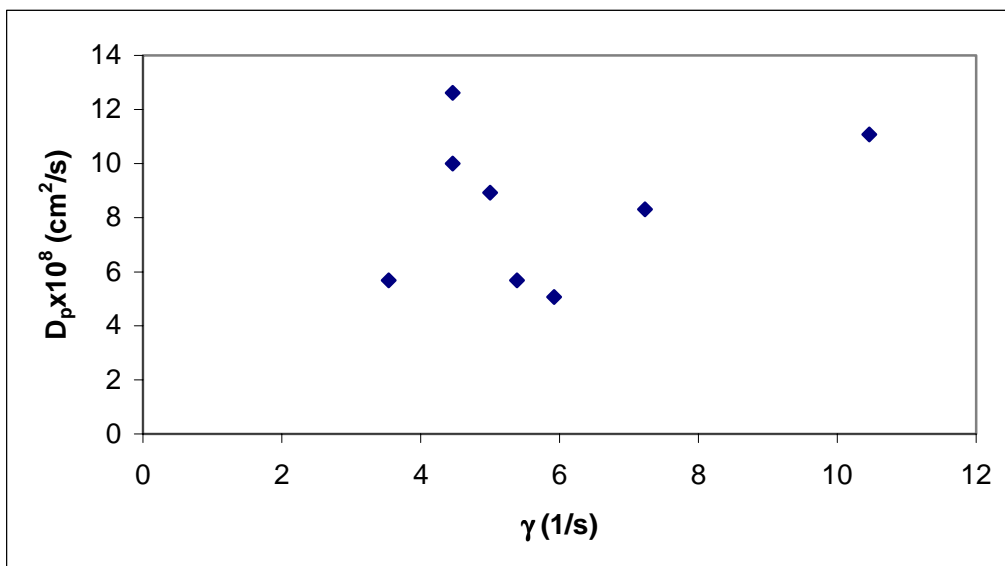


Figure B.2. Experimental results of Goldsmith and Marlow (1979) for the dispersion of red blood cells at  $\bar{h} = 0.4$ .

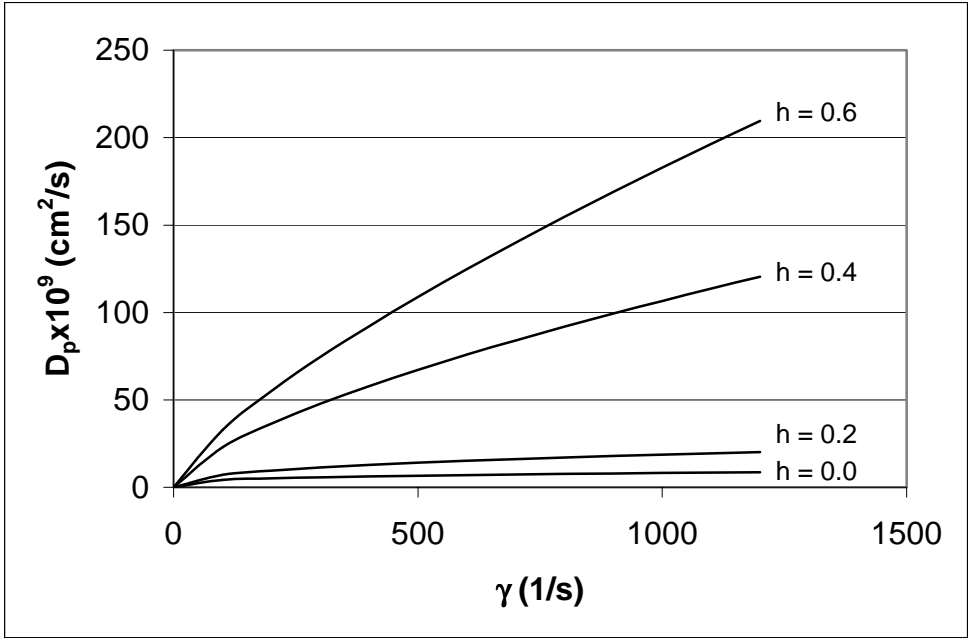


Figure B.3. Empirical correlation of Aarts et al (1986) for the diffusivity of platelets at various mean hematocrits.

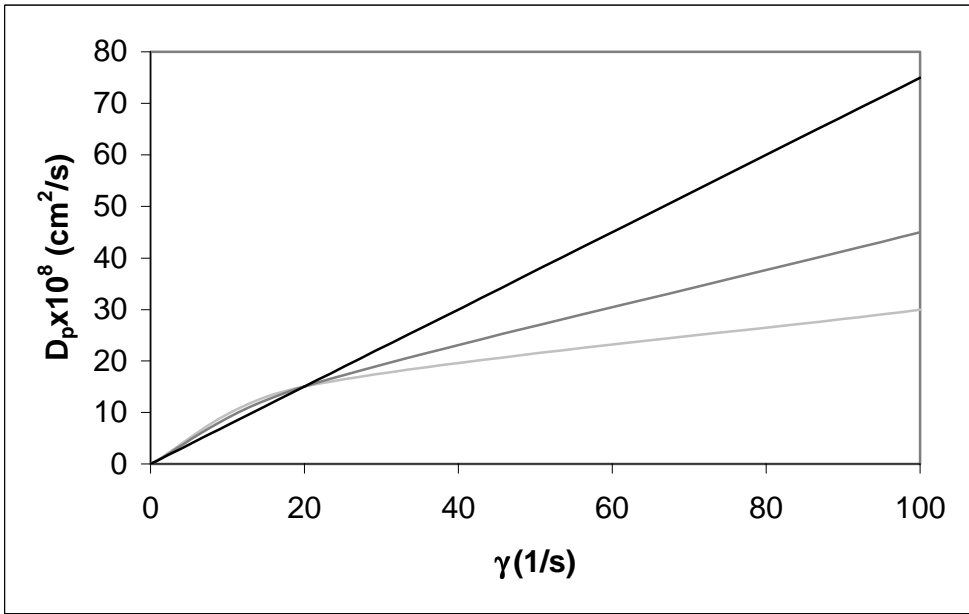


Figure B.4. Sample of curves possible for a shear based model of monocyte dispersion. All curves pass through the single experimental observation of Goldsmith and Karino (1974) at  $\dot{\gamma} \approx 20 \text{ s}^{-1}$ .